mRNA and lncRNA expression profiles of liver tissues in children with biliary atresia

WENYAN WU[1,2*], WEIFANG WU[3,4*], YONGQIN YE[4,5], TAO LI[2] and BIN WANG[4]

[1]Medical Laboratory, Shenzhen Luohu People's Hospital, Shenzhen, Guangdong 518001; [2]Guangdong Provincial Key Laboratory of Medical Molecular Diagnostics, Guangdong Medical University, Dongguan, Guangdong 523000; [3]Medical College, Shantou University Medical College, Shantou, Guangdong 515041; [4]Department of General Surgery, Shenzhen Children's Hospital, Shenzhen, Guangdong 518026; [5]Faculty of Medicine, Macau University of Science and Technology, Macau SAR 999078, P.R. China

Received May 18, 2022; Accepted August 1, 2022

DOI: 10.3892/etm.2022.11571

Abstract. Progressive liver fibrosis is the most common phenotype in biliary atresia (BA). A number of pathways contribute to the fibrosis process so comprehensive understanding the mechanisms of liver fibrosis in BA will pave the way to improve patient's outcome after operation. In this study, the differentially expressed profiles of mRNAs and long non-coding RNAs from BA and choledochal cyst (CC) liver tissues were investigated and analyzed, which may provide potential clues to clarify hepatofibrosis mechanism in BA. A total of two BA and two CC liver tissue specimens were collected, the expression level of mRNAs and lncRNAs was detected by RNA sequencing. Differentially expressed mRNAs (DEmRNAs) were functionally annotated and protein-protein interaction networks (PPI) was established to predict the biological roles and interactive relationships. Differentially expressed lncRNAs (DElncRNAs) nearby targeted DEmRNA network and DElncRNA-DEmRNA co-expression network were constructed to further explore the roles of DElncRNAs in BA pathogenesis. The expression profiles of significant DEmRNAs were validated in Gene Expression Omnibus database. A total of 2,086 DEmRNAs and 184 DElncRNAs between BA and CC liver tissues were obtained. DEmRNAs were enriched in 521 Gene Ontology terms and 71 Kyoto Encyclopedia of Genes and Genomes terms which were mainly biological processes and metabolic pathways related to immune response and inflammatory response. A total of five hub proteins (TYRO protein tyrosine kinase binding protein, C-X-C motif chemokine ligand 8, pleckstrin, Toll-like receptor 8 and C-C motif chemokine receptor 5) were found in the PPI networks. A total of 31 DElncRNA-nearby-targeted DEmRNA pairs and 2,337 DElncRNA-DEmRNA co-expression pairs were obtained. The expression of DEmRNAs obtained from RNA sequencing were verified in GSE46960 dataset, generally. The present study identified key genes and lncRNAs participated in BA associated liver fibrosis, which may present a new avenue for understanding the patho-mechanism for hepatic fibrosis in BA.

Introduction

Biliary atresia (BA) is a rare but severe neonatal disease characterized by an inflammatory and progressive fibrotic obstruction of the extrahepatic bile ducts resulting in cholestasis and subsequent hepatic failure if left untreated (1). Rapid liver fibrosis is a major outcome for children with BA even though they might appear normal at birth (2,3). Knowledge on the pathogenesis of liver fibrosis in BA is still limited. Considering the complicated etiologies, the identify potentially modifiable factors in BA associated liver fibrosis is an urgent need (2).

The microarray and RNA-seq technique can help to identify signatures of predominant transcriptions of the liver during fibrosis progressive in BA, which could be beneficial for uncovering new molecular mechanisms to improve the prognosis, diagnosis and treatment of this disease (4). This technique has been successfully applied for liver tissues from BA and CC to investigate the potential underlying mechanism (5-8). A transcriptional analysis of liver tissues from BA and CC identified 877 differentially expressed genes (such as COX1, SCO2, and CYTB, which are involved in oxidative phosphorylation) and several pathways with immune and inflammatory responses involved in the pathogenesis of BA (such as the Wnt-signaling pathway and TGF-β pathway) (5) Previous studies have found that the NF-κB signaling pathway could regulate genes related to immune response and mediate liver fibrosis by initiating fibrosis factors and thus might serve a key role in the development of BA (9-11). Another RNA sequencing of livers from 6 BA and 6 CC found that Foxa3 may exert a role in the progression of hepatic fibrosis in BA, which may

Correspondence to: Professor Bin Wang, Department of General Surgery, Shenzhen Children's Hospital, 7019 Yitian Road, Futian, Shenzhen, Guangdong 518026, P.R. China
E-mail: szwb1967@126.com

*Contributed equally

Key words: biliary atresia, liver fibrosis, mRNA, long non-coding RNA, bioinformation analysis

be a potential targeted treatment (6). Fas ligand mRNA (7), MMP7 and PCK1 (8) can be used as potential biomarkers to predict the outcome of BA and the fibrosis progression. A comparison of mRNA expression level from normal, diseased control and end-stage BA livers identified 35 genes involved in cell signaling, transcription regulation, hepatobiliary development and fibrosis process (12). The expression level of genes regulating fibrosis in liver tissues increases in infants who survived within 2 years (13). Furthermore, cDNA array demonstrate two hepato-fibrogenesis-associated genes (4), plasminogen activator inhibitor-1 (PAI-1) and tissue inhibitor of metalloproteinase-1 (TIMP-1).

Long noncoding RNAs (lncRNAs) exert specific regulatory functions in various cellular organization (14), which are involved in hepatic fibrosis by regulating gene or protein expression (15). LncRNAs can act as competing endogenous RNAs (ceRNAs) to participate in hepatic fibrosis (16). The expression level of long noncoding RNA H19 (lncRNA H19) is positively correlated with the severity of fibrotic liver injuries in BA patients, which serves a pivotal role in BA cholangiocyte proliferation and cholestatic liver injury as a sponge for let-7/HMGA2 axes and regulates S1PR2/SphK2 (17). LncRNA-Annexin A2 pseudogene 3 (ANXA2P3) is identified to participate in the process of BA-induced liver fibrosis by regulating Annexin A2 (ANXA2) (18). Our previous study on lncRNA-adducin 3 antisense RNA1 was identified as participating in liver fibrosis by targeting ADD3 *in vitro* accelerating the proliferation and migration of LX-2 cells, which are the key cells involved in hepatic fibrosis (19). The construction and analysis of regulation network based on microarray and RNA-seq results can improve understanding of the mechanisms underlying BA associated hepatic fibrosis. More evidence will pave the way to fully understand hepatic fibrosis pathogenesis in BA patients (20).

The present study aimed to identify some key DEmRNAs and DElncRNA in liver tissues of BA patients through RNA-sequencing and also to discover some hub proteins via constructing PPI networks of DEmRNAs and DElncRNA-DEmRNA co-expression networks. Through the aforementioned approaches, it was expected to ascertain some lncRNAs, mRNAs and pathways that serve an important role in the pathogenesis of liver fibrosis with BA.

Materials and methods

Patient samples. The present study was approved by Ethics Committee on Human Research of Shenzhen Children's Hospital (approval no. 202106602) and was conducted in accordance with the principles expressed in the 1975 Declaration of Helsinki. A total of two BA infants and two age-matched choledochal cyst (CC) infants with a normal liver function were included in the present study. All the enrolled infants were confirmed diagnosed intraoperative cholangiography by the same surgical group in Shenzhen Children's Hospital. Liver biopsy tissues were collected with a written informed consent from all infants' guardians. The patient's clinical information is presented in Table I.

Table I. Clinical information in infants with BA and CC.

Variable	BA-1	BA-2	CC-1	CC-2
Age, days	72	50	1,095	857
Sex	Male	Male	Female	Female
ALP, IU/L	771	569	326	160
ALT, IU/L	37	85	52	14
AST, IU/L	196	177	57	29
TBIL, μmol/l	193.5	119.9	7.4	5.4
DBIL, μmol/l	104,2	69.8	1.2	1.1
GGT, IU/l	422	938	90	13

BA, biliary atresia; CC, choledochal cyst; ALP, Alkaline phosphatase; ALT, alanine transaminase; AST, aspartate transaminase; TBIL, total bilirubin; DBIL, direct bilirubin; GGT, gamma-glutamyl transferase.

RNA isolation and sequencing. Total RNA was extracted from liver tissue samples using TRIzol® (Thermo Fisher Scientific, Inc.). Nanodrop (Thermo Fisher Scientific, Inc.) was used for preliminary qualification and quantification of RNA concentration and Agilent 2100 (Agilent Technologies, Inc.) was used for precise detection of quality of RNA library. Agarose gel electrophoresis was used to detect the integrity of retracted RNA.

After the RNA samples were qualified, rRNA was removed with Ribo-zero kit (EpiCentre; Illumina, Inc.) and then the RNA was fragmented under high temperature and metal ions. Using ribosomal-depleted RNA as a template, first-strand cDNA was synthesized with random hexamers. Subsequently, second-stranded cDNA was synthesized by adding buffer, dNTPs (dUTP, dATP, dGTP and dCTP) and enzymes, followed by purification of double-stranded cDNA using VAHTSTM DNA Clean Beads (Vazyme Biotech Co., Ltd.). The final strand-specific cDNA library was obtained through a series of experiments such as end repair, tailing, sorting, digestion of cDNA containing U by using UDG enzyme and PCR enrichment. Illumina HiSeq X Ten platform (Illumina, Inc.) sequencing was performed after pooling different libraries according to the requirements of effective concentration and target data volume. The processing and database construction for RNA-seq are in Fig. S1 and Appendix S1.

Identification of DEmRNAs and DElncRNAs. The reference sequences of the corresponding species were downloaded from the database Ensemble GRCh38.p7 (ftp://ftp.ncbi.nlm.nih.gov/genomes/Homo_sapiens) for comparison with the sequencing data. Expression of mRNAs and lncRNAs was normalized and outputted with StringTie version 1.3.3b (http://ccb.jhu.edu/software/stringtie/). |log2FC|>1 and P<0.05 were used as the cut-off criteria. Volcano plots and hierarchical clustering were used to visualize the overall distribution of differential transcripts.

Functional annotation and pathway enrichment of DEmRNAs. DAVID (https://david.ncifcrf.gov) is an online database that aggregates large numbers of genes or proteins into corresponding functional annotations and pathways, providing a quick access to various annotation data. P<0.05 was used

Table II. Top 10 up- and downregulated DEmRNAs between BA liver tissues and CC liver tissues.

ID	Symbol	log2FC	P-value	Regulation
ENSG00000244734	HBB	6.99799	$5.00x10^{-5}$	Up
ENSG00000147257	GPC3	5.86627	$5.00x10^{-5}$	Up
ENSG00000159217	IGF2BP1	5.61870	$5.00x10^{-5}$	Up
ENSG00000081051	AFP	5.41660	$5.00x10^{-5}$	Up
ENSG00000068366	ACSL4	5.21616	$5.00x10^{-5}$	Up
ENSG00000276368	HIST1H2AJ	4.71279	$5.00x10^{-5}$	Up
ENSG00000169213	RAB3B	4.47424	$5.00x10^{-5}$	Up
ENSG00000274267	HIST1H3B	4.37440	$5.00x10^{-5}$	Up
ENSG00000115009	CCL20	4.33093	$5.00x10^{-5}$	Up
ENSG00000274641	HIST1H2BO	4.25590	$5.00x10^{-5}$	Up
ENSG00000140505	CYP1A2	-7.78389	$5.00x10^{-5}$	Down
ENSG00000117594	HSD11B1	-5.94395	$5.00x10^{-5}$	Down
ENSG00000122787	AKR1D1	-4.81138	$5.00x10^{-5}$	Down
ENSG00000124713	GNMT	-4.80215	$5.00x10^{-5}$	Down
ENSG00000180875	GREM2	-4.63967	$5.00x10^{-5}$	Down
ENSG00000160868	CYP3A4	-4.56139	$5.00x10^{-5}$	Down
ENSG00000205362	MT1A	-4.36469	$5.00x10^{-5}$	Down
ENSG00000134760	DSG1	-4.21303	$5.00x10^{-5}$	Down
ENSG00000171234	UGT2B7	-4.15848	$5.00x10^{-5}$	Down
ENSG00000166415	WDR72	-4.11164	$5.00x10^{-5}$	Down

DEmRNAs, differentially expressed mRNAs; FC, fold change.

as the cutoff criterion for Gene Ontology (GO) functional enrichment analysis and Kyoto Encyclopedia of Genes and Genomes (KEGG) pathway enrichment analysis.

Protein-protein interaction (PPI) networks construction. The STRING protein interaction database (http://string-db.org/) and the R language (http://www.R-project.org/) package STRINGdb were used for Top 100 up- and downregulated DEmRNAs protein interaction network analysis. Cytoscape software (version 3.5.0, http://www.cytoscape.org) was applied to visualize PPI networks.

Nearby-targeted DEmRNAs of DElncRNAs. The functions of lncRNAs may be related to their adjacent protein-coding mRNAs (21,22), so the protein-coding mRNAs (100-kb upstream and downstream) adjacent to lncRNAs were selected as their target mRNAs. The lncRNA-mRNA regulated networks were visualized by Cytoscape software (version 3.5.0, http://www.cytoscape.org).

DElncRNA-DEmRNA co-expression networks. DElncRNA-DEmRNA co-expression was calculated based on the dynamic changes of lncRNA and mRNA expression signal values, including expression regulation relationship and regulation direction. The DElncRNA-DEmRNA pairs with absolute values of PCC >0.99 and P<0.01 were selected and DElncRNA-DEmRNA co-expression network was constructed and visualized by Cytoscape software (version 3.5.0, http://www.cytoscape.org). Functional annotation and Pathway Enrichment of the DEmRNAs co-expressed with DElncRNAs were performed with DAVID. P<0.05 was used as the criterion.

Validation in the Gene Expression Omnibus (GEO) dataset. The mRNA expression profiles (GSE46960) was downloaded from the GEO database (https://www.ncbi.nlm.nih.gov/geo/), which included a collection of 64 liver biopsy sample obtained from a patient with BA (case group) and 7 liver biopsy sample obtained from a deceased-donor adult (normal group). The expression of screened DEmRNAs obtained from our RNA sequencing were verified using the GSE46960 dataset.

Statistical analysis. Sequencing data were analyzed by using fold changes (FC) and Student's t-test. |log2FC|>1 and P<0.05 were set as the criterion to identify the differentially expressed mRNAs and lncRNAs.

Results

DEmRNAs and DElncRNAs between BA liver tissues and CC liver tissues. There were 2,086 DEmRNAs (1,036 up- and 1,050 downregulated) and 184 DElncRNAs (52 up- and 132 downregulated) in the BA group. The top 10 upregulated and downregulated DEmRNAs and DElncRNAs are in Tables II and III. Volcano maps of DEmRNAs and DElncRNAs are in Fig. 1A and B, respectively. Hierarchical clustering of DEmRNAs and DElncRNAs is shown in Fig. 1C and D. The raw data of the sequencing data of the present study have been uploaded to Sequence Read Archive (SRA) for SUB7923751 at https://www.ncbi.nlm.nih.gov/sra/PRJNA701623.

Table III. Top 10 up- and downregulated DElncRNAs between BA liver tissues and CC liver tissues.

ID	Symbol	log2FC	P-value	Regulation
ENSG00000260604	RP1-140K8.5	2.61436	$5.00x10^{-5}$	Up
ENSG00000281508	CDR1-AS	2.19782	$5.00x10^{-5}$	Up
ENSG00000270507	CTA-21C21.1	3.44985	0.00010	Up
ENSG00000232931	LINC00342	1.56982	0.00435	Up
ENSG00000259834	RP11-284N8.3	1.59598	0.00665	Up
ENSG00000225470	JPX	25.47320	0.00705	Up
ENSG00000277152	RP11-622C24.2	1.55379	0.00765	Up
ENSG00000214049	UCA1	3.00640	0.00990	Up
ENSG00000267731	RP11-147L13.8	1.79259	0.01435	Up
ENSG00000172965	MIR4435-2HG	1.87816	0.01525	Up
ENSG00000230645	AC016682.1	-4.03424	$5.00x10^{-5}$	Down
ENSG00000261578	RP11-21L23.2	-3.94999	$5.00x10^{-5}$	Down
ENSG00000250056	LINC01018	-2.43565	0.00070	Down
ENSG00000248709	CTC-505O3.2	-3.32413	0.00100	Down
ENSG00000236378	RP11-394G3.2	-8.03214	0.00115	Down
ENSG00000234509	AP000253.1	-3.26890	0.00145	Down
ENSG00000251637	RP11-119D9.1	-3.81996	0.00275	Down
ENSG00000261012	RP11-116D2.1	-1.07168	0.00285	Down
ENSG00000260855	RP11-439E19.10	-1.57691	0.00395	Down
ENSG00000234456	MAGI2-AS3	-2.02662	0.00420	Down

DElncRNAs, differentially expressed lncRNAs; FC, fold change.

Functional annotation of DEmRNAs. To improve understanding of the biological functions of DEmRNAs, GO and KEEG enrichment analyses were performed. Oxidation-reduction process ($P=1.52x10^{-21}$), immune response ($P=3.10x10^{-17}$), inflammatory response ($P=4.12x10^{-16}$) and metabolic process ($P=1.09x10^{-11}$) were significantly enriched GO biological process in BA (Fig. 2A). Extracellular exosome ($P=3.47x10^{-45}$) and mitochondrial matrix ($P=1.35x10^{-18}$) were significantly enriched GO cellular component in BA (Fig. 2B) Electron carrier activity ($P=5.30x10^{-16}$) and pyridoxal phosphate binding ($P=1.14x10^{-12}$) were significantly enriched GO molecular function in BA (Fig. 2C). Metabolic pathways ($P=4.63x10^{-18}$), Biosynthesis of antibiotics ($P=5.88x10^{-17}$), Glycine, serine and threonine metabolism ($P=2.19x10^{-13}$) and complement and coagulation cascades ($P=3.19x10^{-12}$) were top 4 enriched KEGG pathways in BA (Fig. 2D).

Protein-protein interaction (PPI) networks. The PPI networks contained 176 nodes and 665 edges. TYRO protein tyrosine kinase binding protein (degree=29), C-X-C motif chemokine ligand 8 (degree=27), Toll-like receptor (TLR) 8 (degree=24), pleckstrin (degree=23), C-C motif chemokine receptor (CCR)5 (degree=22), CCR1 (degree=22), lysosomal-associated protein transmembrane 5 (degree=21), TLR7 (degree=21), cytochrome P450 family 3 subfamily A member 4 (degree=21) and CD53 molecule (degree=20) were the top 10 hub proteins of the PPI networks (Fig. 3).

DElncRNAs-nearby-targeted DEmRNAs. There were 31 DElncRNAs-nearby-targeted DEmRNA pairs in total, of which 31 DElncRNAs and 30 DEmRNA were detected (Fig. 4). CTD-2256P15.2 and XLOC_045318 all nearby CMBL.

DElncRNA-DEmRNA co-expression networks. There were 2,337 DElncRNA-DEmRNA co-expression pairs in total, of which 54 DElncRNAs and 848 DEmRNAs were identified with an absolute value of PCC >0.99 and P<0.01 (Fig. 5). The positive regulated network is shown in Fig. 5A and the negative regulated network shown in Fig. 5B and C.

Functional annotation of DEmRNAs co-expressed with DElncRNAs. Inflammatory response ($P=1.04x10^{-12}$), immune response ($P=1.64x10^{-09}$), neutrophil chemotaxis ($P=3.03x10^{-08}$) and oxidation-reduction process ($P=1.85x10^{-07}$) were significantly enriched GO terms (Fig. 6A). Extracellular exosome ($P=2.14x10^{-24}$) and plasma membrane ($P=2.16x10^{-10}$) were significantly enriched GO cellular component in BA (Fig. 6B). Oxidoreductase activity ($P=3.77x10^{-05}$) and aldehyde dehydrogenase activity ($P=6.74x10^{-05}$) were significantly enriched GO molecular function in BA (Fig. 6C). Complement and coagulation cascades ($P=2.57x10^{-07}$), Fatty acid degradation ($P=2.85x10^{-06}$), Drug metabolism-cytochrome P450 ($P=1.20x10^{-04}$) and Metabolic pathways ($P=2.68x10^{-04}$) were top 4 significantly enriched KEGG pathways (Fig. 6D).

Validation of selected DEmRNAs in GEO database. An mRNA expression profile was downloaded from GEO database and the expression patterns of DEmRNAs obtained from our RNA sequencing were verified. As shown in Fig. 7A and B, 111 mRNAs in upregulated DEmRNAs and

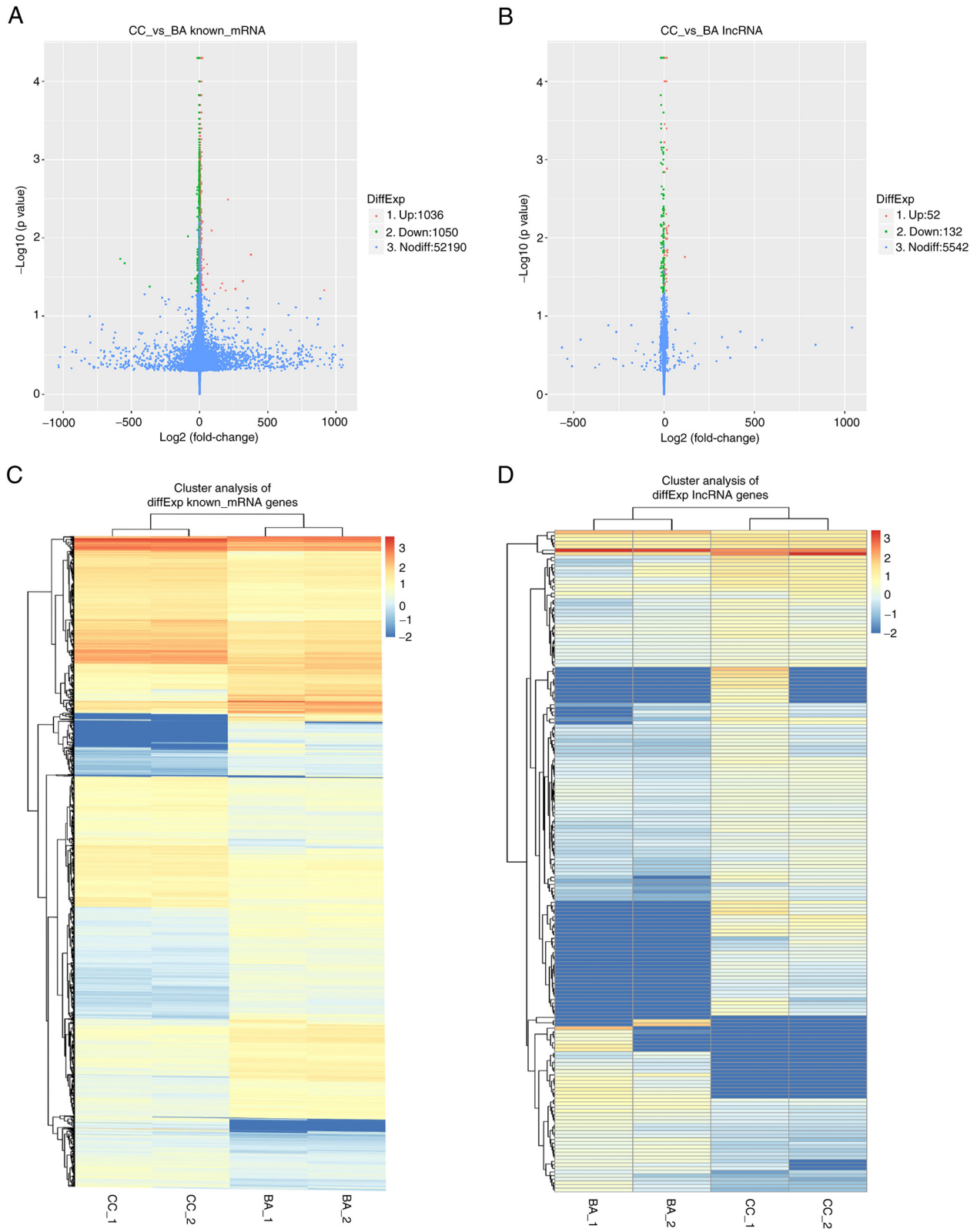

Figure 1. DEmRNAs and DElncRNAs between BA liver tissues and CC liver tissues. Volcano spot results of (A) DEmRNAs and (B) DElncRNAs between BA liver tissues and CC liver tissues. Red spot and green spot respectively indicated up- and downregulated genes, blue spot indicated no significant difference. Hierarchical clustering results of (C) DEmRNAs and (D) DElncRNAs between BA liver tissues and CC liver tissues. DEmRNAs/DElncRNAs and tissue samples were displayed as row and column, respectively. The color scale represented the expression levels. DEmRNAs, differentially expressed mRNAs; DElncRNAs, differentially expressed lncRNAs; BA, biliary atresia; CC, choledochal cyst.

102 mRNAs in downregulated DEmRNAs were verified. Then when the present study focused on the top 10 upregulated DEmRNAs in BA from the results (Table II), five of them (HBB, GPC3, IGF2BP1, AFP and CCL20) were consistent with the GEO database in terms of expression patterns of mRNA (Fig. 7C). Similarly, mRNAs of CYP1A2, HSD11B1,

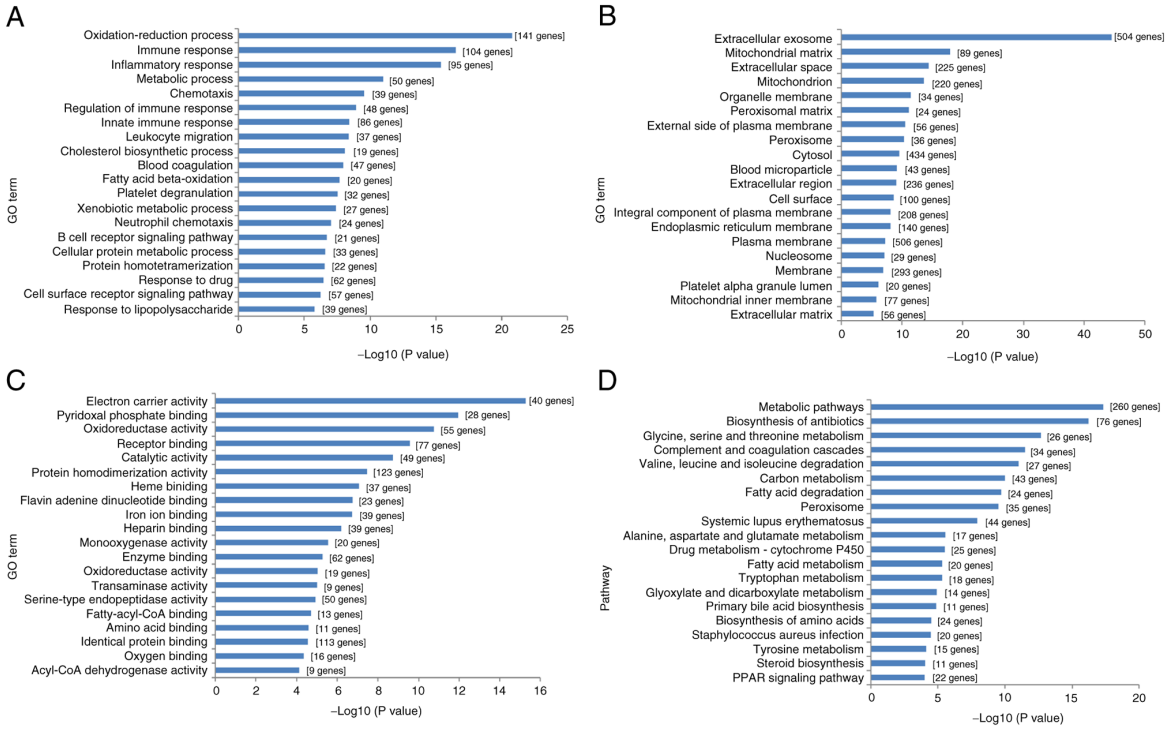

Figure 2. Top 20 significantly enriched GO terms and top 20 KEGG pathways of DEmRNAs between BA liver tissues and CC liver tissues. The x-axis is p-value for each GO term or pathway as -log10 and the y-axis indicates (A) biological process GO term, (B) cellular component GO term, (C) molecular function GO term or (D) KEGG pathway. GO, Gene Ontology; KEGG, Kyoto Encyclopedia of Genes and Genomes; DEmRNAs, differentially expressed mRNAs; BA, biliary atresia; CC, choledochal cyst.

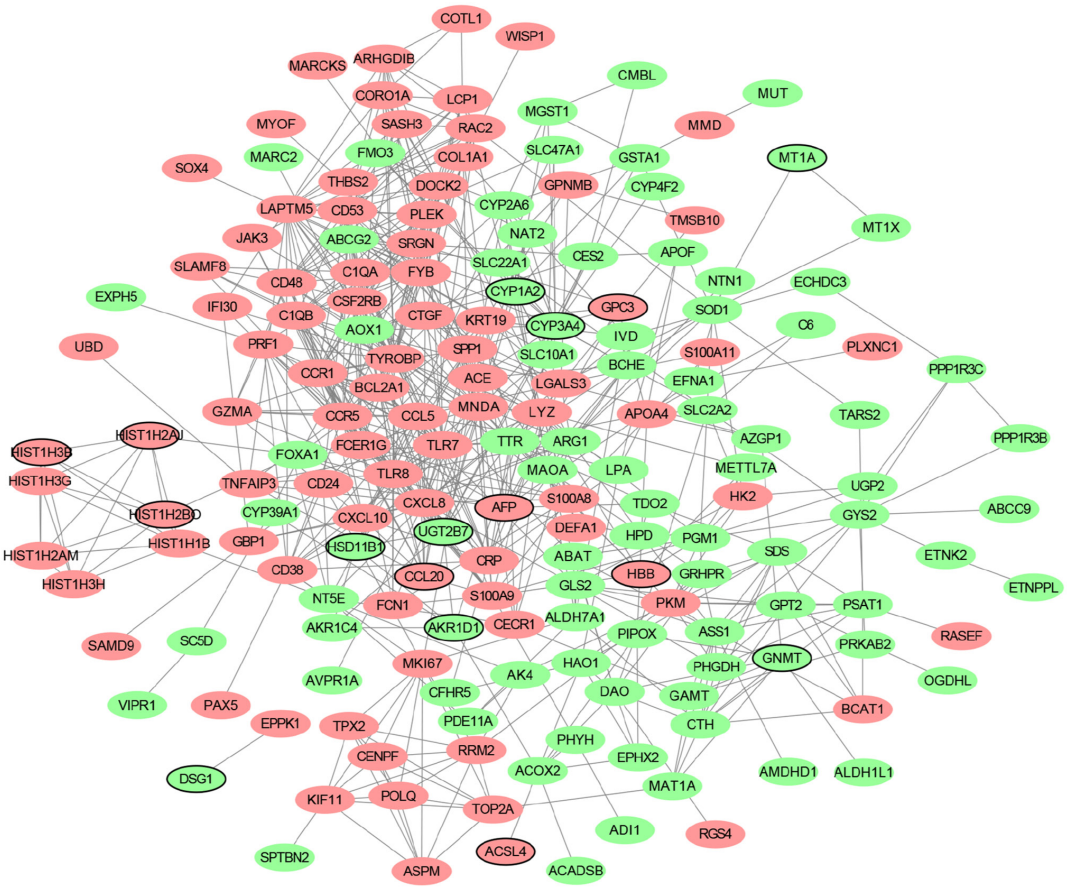

Figure 3. PPI networks. Proteins encoded by up- and downregulated DEmRNAs between BA liver tissues and CC liver tissues were displayed as red and green ellipses. DEmRNAs derived from top 10 up- and downregulated DEmRNAs between BA liver tissues and CC liver tissues were displayed in ellipses with a black border. PPI, protein-protein interaction; DEmRNAs, differentially expressed mRNAs; BA, biliary atresia; CC, choledochal cyst.

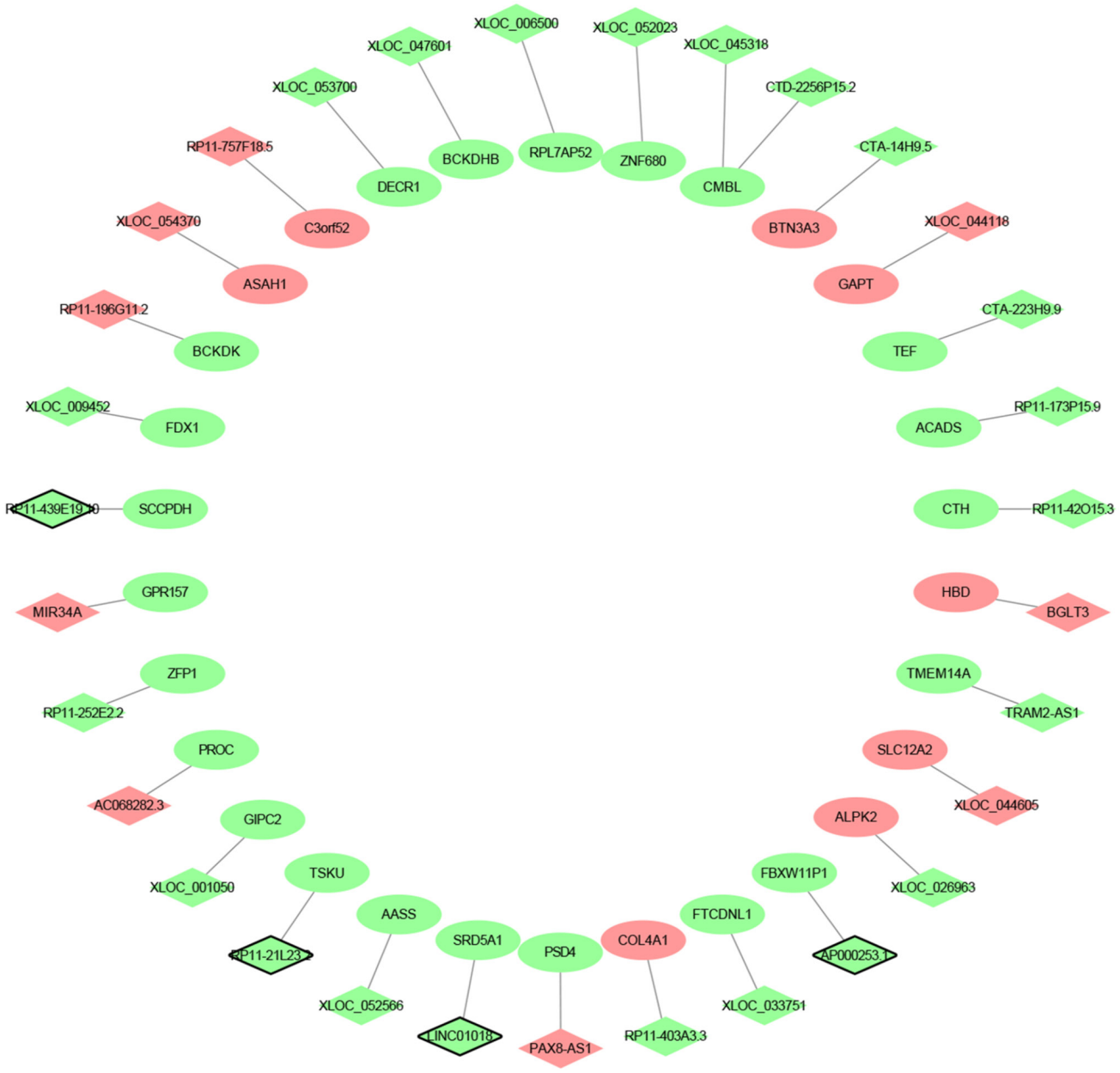

Figure 4. DElncRNA-nearby DEmRNA interaction networks. DElncRNAs and their nearby DEmRNAs between BA liver tissues and CC liver tissues, respectively, were represented in the rhombus and ellipses. up- and downregulation of DEmRNAs in BA liver tissues compared with CC were shown in red and green color, respectively. DElncRNAs/DEmRNAs derived from top 10 up- and downregulated DElncRNAs/DEmRNAs were displayed in rhombus and ellipses with a black border. DElncRNAs, differentially expressed lncRNAs; DEmRNAs, differentially expressed mRNAs; BA, biliary atresia; CC, choledochal cyst.

AKR1D1, GNMT, MT1A and WDR72 were shown to be lower-expressed in the GEO database, which were consistent with the top 10 downregulated DEmRNAs from the results (Table II and Fig. 7D).

Discussion

Hepatic fibrosis usually develops in a progressive pattern in infants with BA. Even though these patients received Kasai portoenterostomy (KPE), the majority of them still have to undergo liver transplant due to severe fibrosis, cirrhosis and liver failure. However, the molecular network underpinning this expeditious fibrogenic process remains to be elucidated (23). In this regard, the present study performed RNA sequencing on liver samples of BA and CC to identify abundant DElncRNAs and DEmRNAs between two groups.

First, the results were analyzed for mRNA and lncRNA that were significantly upregulated or downregulated, including GPC3, AFP, CYP1A2, CCL20, 11βHSD1, AKR1D1, GNMT, JPX and MIR4435-2HG.

Glypican-3 (GPC3) a heparan sulfate proteoglycan attached to the cell membrane, serves a role in the regulation of the signaling activity involved in numerous growth factors (24), including Wnt/β (25), Hedgehogs (26), bone morphogenetic proteins and fibroblast growth factors (27). The Wnt/β-catenin signaling pathway has a key role in the regulation of cellular functions such as biliary cell fate (28), thereby raising a potential participation in BA etiology via GPC3-mediated

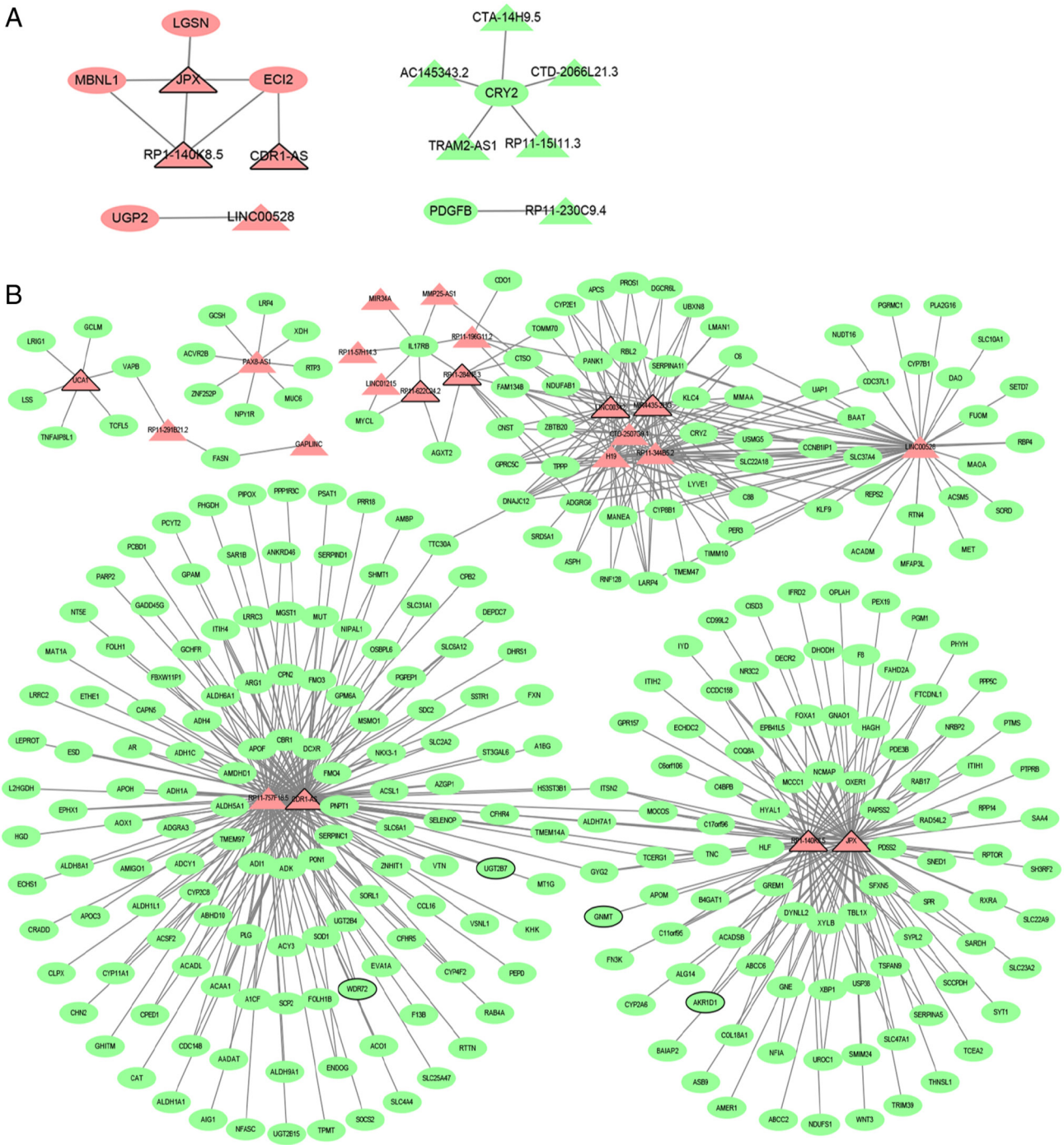

Figure 5. Continued.

Wnt/β-catenin signaling. Sirisomboonlarp *et al* (29) found that circulating GPC3 protein is significantly elevated in BA patients and positively correlated with liver stiffness, indicating that serum GPC3 could be a biomarker to evaluate hepatic function and to predict prognosis for BA patients following Kasai surgery. Notably, from the results of the present study, GPC3 was also identified to be the second most over-expressed DEmRNAs in BA liver tissues.

Serum α-fetoprotein (AFP) was strongly associated with epithelial liver tumors (30). It has a sensitivity of >90 and >70%, for hepatocellular carcinoma and hepatoblastoma (HB), respectively (31). Amir *et al* (32) found that patients with BA are far more prone to suffer from HB and in such cases, serum AFP levels might not be specific to diagnose HB in such cases, though remaining sensitive. A previous study (33) identified that ~8% of BA children were affected by liver tumors and AFP level screening and regular imaging examinations were crucial for early diagnosis of malignant liver tumors in BA patients.

Distinguishing BA from other non-BA neonatal cholestasis is challenging (34). Shteyer *et al* (35) show that Continuous Breath 13C-methacetin breath test might be useful to distinguish BA from non-BA. Methacetin is a substrate that can evaluate liver metabolic function by being metabolized by cytochrome P450 1A2 (CYP1A2) (36), which is negatively

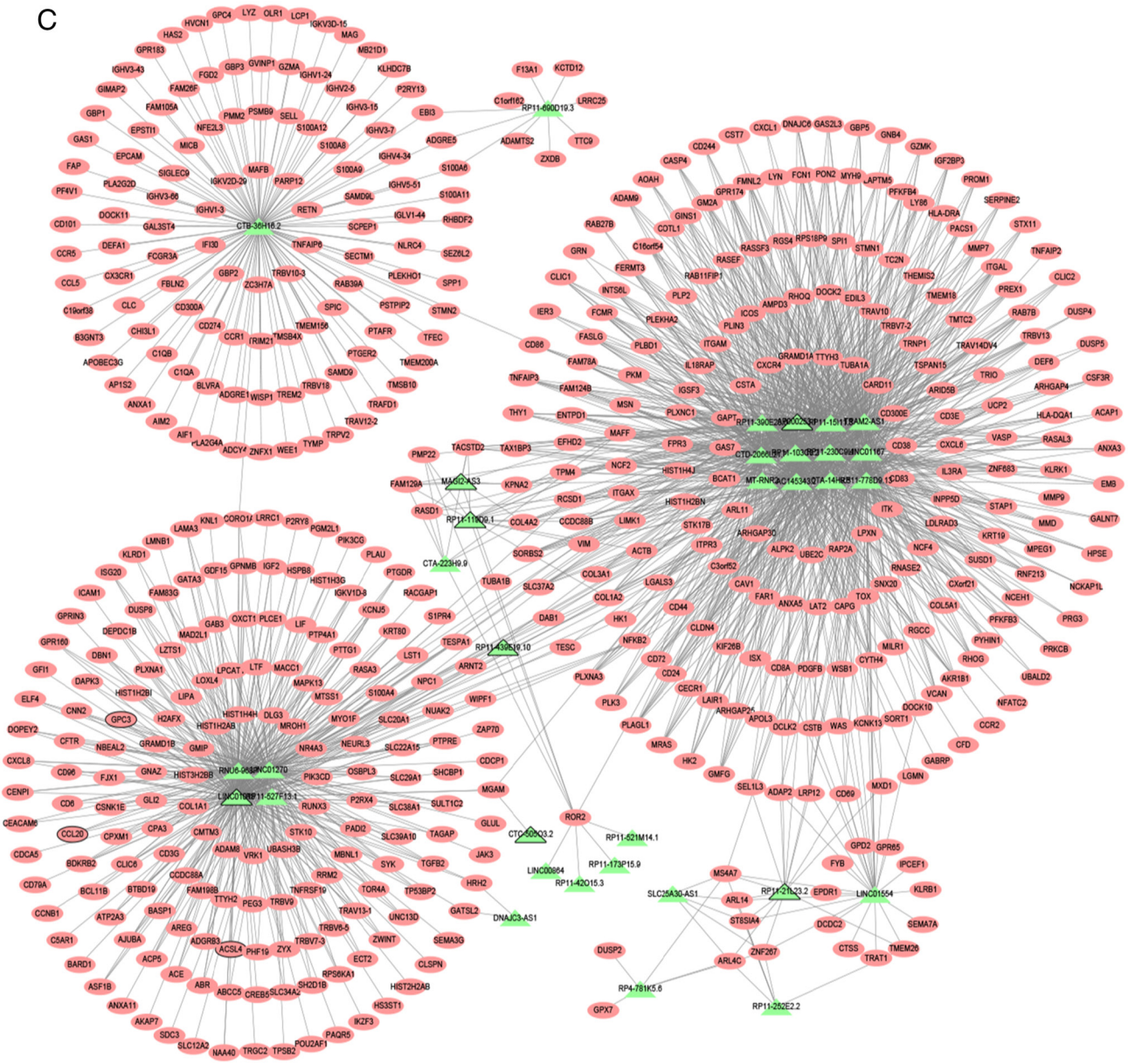

Figure 5. DElncRNA-DEmRNA co-expression networks, including (A) positive regulatory and negative regulated networks. (B and C). DElncRNAs and their nearby DEmRNAs between BA liver tissues and CC liver tissues were shown in triangles and ellipses, respectively. Up- and downregulation in BA liver tissues compared with CC liver tissues were displayed in red and green color, respectively. DElncRNAs/DEmRNAs derived from top 10 up- and downregulated DElncRNAs/DEmRNAs were displayed in triangles and ellipses with a black border. DElncRNAs, differentially expressed lncRNAs; DEmRNAs, differentially expressed mRNAs; BA, biliary atresia; CC, choledochal cyst.

correlated with hepatic fibrosis in patients with chronic hepatitis C viral infection (37,38) and is also found to be involved in other forms of hepatic diseases (39). Crawford *et al* (40) discovered that downregulated CYP1A2 could aggravate inflammatory response due to an increase of proinflammatory cytokines, such as TNF-α and IL-6. CYP1A2 is the most significant downregulated DEmRNAs in BA liver tissues, indicating that it might participate in this inflammatory fibrosclerosing disease and thus can be an indicator to differentiate BA. Therefore, further investigations into the intrinsic pathway of CYP1A2 on the etiology of progressive fibrosis in BA are of importance.

It is hypothesized that the discovery of more valuable biomarkers to monitor the progression of hepatic fibrosis following KPE may help improve clinical outcomes in patients and delay the need for liver transplantation (41), including lncRNA APTR (42), miR-21 (43) and mRNA FN14 (44). In the present study, the results also identified a number of valuable biomarkers related to liver fibrosis. Chemokine ligand-20 (CCL20) acted as a potent chemoattractant for immature dendritic cells, which can mediate the strong inflammatory responses that drive liver fibrosis (45). *In vivo* experiments show that a deficiency of 11β-hydroxysteroid dehydrogenase-1 (11βHSD1) could lead to the activation of hepatic myofibroblast and thus exacerbate liver fibrosis in mice (46). Expression level of steroid 5β-reductase (AKR1D1) in the liver tissue is negatively correlated with liver fibrosis and inflammation (47). Glycine N-methyltransferase (GNMT) is the most abundant

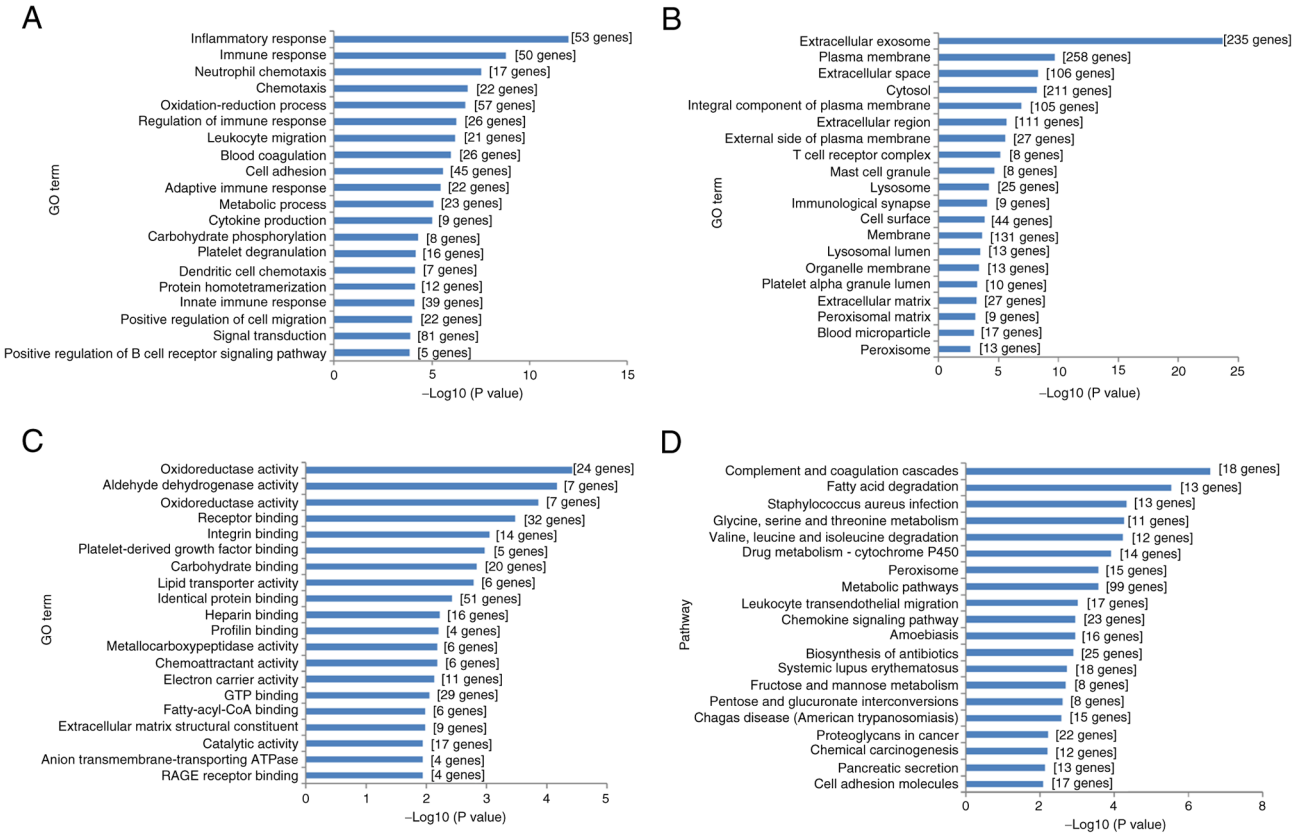

Figure 6. Top 20 significantly enriched GO terms and KEGG pathways of DEmRNAs co-expressed with DElncRNAs between BA liver tissues and CC liver tissues. The x-axis is P-value for each GO term or pathway as -log10 and the y-axis indicates (A) biological process GO term, (B) cellular component GO term, (C) molecular function GO term or (D) KEGG pathway. GO, Gene Ontology; KEGG, Kyoto Encyclopedia of Genes and Genomes; DEmRNAs, differentially expressed mRNAs; BA, biliary atresia; CC, choledochal cyst.

methyltransferase in the liver and its reduction has a negative effect on the maintenance of normal liver functions progressing to fibrosis, cirrhosis and hepatocellular carcinoma (48).

Liver fibrosis is strongly associated with the activation of hepatic stellate cells. LncRNA XIST enhances eol-induced autophagy process and subsequently activates hepatic stellate cells through the miR-29b/HMGB1 signaling pathway (49). LncRNA JPX, a non-protein coding RNA transcribed by the X deactivated central gene, activates XIST transcription via an interaction with CCCTC-binding factor (50). From the sequencing data, the present study identified that JPX was an upregulated DElncRNA. Although the regulatory relationship between JPX and XIST was established, the role it serves in hepatic fibrosis and BA remains to be explored in the future.

Kerola *et al* (51) found a decrease of the expression level of TGF-β1 after successful HPE, indicating that TGF-β1 might be involved in exacerbating liver fibrosis. LncRNA miR4435-2HG can promote prostate carcinoma (52), non-small-cell lung carcinoma (53) and ovarian carcinoma (54) by interacting with TGF-β signaling and thus lncRNA miR4435-2HG-mediated TGF-β1 signaling pathway might be involved in liver fibrosis of BA.

Second, Cytoscape was used to select the top 10 hub genes of PPI network for further analysis and it revealed that CXCL8, TLR8, CCR5, TLR7 and CYP3A4 were associated with BA, revealing that these hub genes may be involved in the occurrence of BA.

CXCL8 regulates inflammation and immune response via chemoattractance to neutrophils (55). Studies show that an elevation of serum CXCL8 together with its increase in liver may participate in inflammation and liver fibrosis in patients with BA and thus CXCL8 may be a potential biomarker for diagnosis, severity evaluation and outcome of BA (56,57).

The major inappropriate host immunological reactions against unknown ligands via the TLR cascades may trigger progressive inflammatory biliary destruction that manifests as BA in newborns or infants. TLR cascades may induce an excessive immune reaction against multiple ligands in the bile duct system, leading to a progressive destruction and inflammatory fibro-obstruction of biliary ducts seen in BA. miR expression level of TLR8 is significantly elevated in liver tissues in the early BA group (58).The activation of TLR7 signaling pathway is crucial for cholangiocytes proliferation in rhesus rotavirus (RRV)-infected mice models (59). In addition, TLR7 can recognize infectious pathogens, activated type 1 interferon and induce the expression of inflammatory response genes, including IL-8 (60).

A previous study has shown that CC chemokines, including CCL2, CCL3, CCL5, stimulate THP-1 cells to increase MMP-9 protein levels in a dose-dependent manner, indicating that the activation of immune cells and MMP are closely related to the occurrence of tissue inflammation (61). Leonhardt *et al* (62) identified >40 significantly differentially-expressed genes in BA mice. Most of the upregulated genes in BA-positive mice

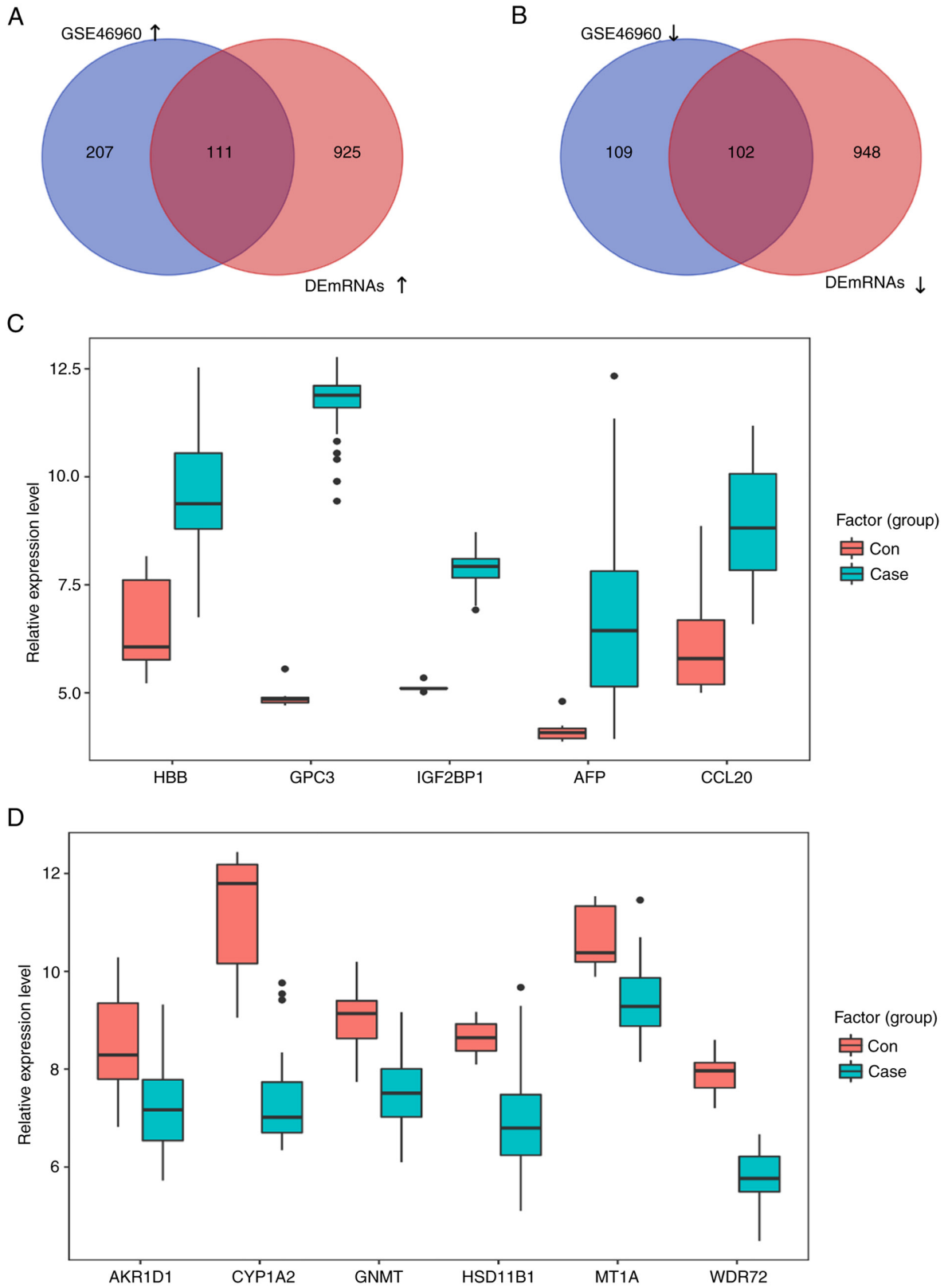

Figure 7. Validation of selected DEmRNAs in GEO database. Venn diagrams indicating that (A) 111 upregulated and (B) 102 downregulated DEmRNAs were consistently in both expression profiles. Boxplot showed (C) 5 upregulated DEmRNAs and (D) 6 downregulated DEmRNAs expression patterns; GEO, Gene Expression Omnibus.

were involved in immune response, such as CCL2, CCL5, CCR5, CXCL9, CXCL10 and IL1F5. To clarify the pathogenesis of BA, the immune reaction during the process of liver fibrosis should be further examined.

Finally, lncRNA-targets were analyzed. In order to fully illustrate how lncRNAs participate in a disease, it is widely accepted to perform a lncRNA-mRNA co-expression analysis to explore the biological functions of lncRNAs by evaluating

and analyzing their co-expressed mRNAs. In the co-expression networks of the present study, CYP2E1 was a target for H19, H19 was upregulated and CYP2E1 was downregulated. Xiao *et al* (17) discovered that the levels of H19 in both liver and serum exosome increase in line with the severity of fibrosis in patients with BA. De Bock *et al* (63) found that CYP1A2, 2C19, 2E1 and 3A4 were at low activity levels in BA patients, which is consistent with the results of the present study. As for how they regulate each other in hepatic fibrosis and BA, this remains to be explored in the future.

A total of 2,086 DEmRNAs and 184 DElncRNAs were identified between liver tissues in BA and CC. DEmRNA and DElncRNA including GPC3, AFP, CYP1A2, CYP3A4, JPX and miR4435-2HG, might have an important role in the pathogenesis of liver fibrosis in BA. Furthermore, the hub genes of PPI network and the relation pairs in the lncRNA-target network were analyzed, including hub gene CXCL8, TLR7, TLR8, CCR5 and lncRNA-target pair H19 CYP2E1.

The mechanisms of fibrogenesis in BA remain to be elucidated, multiple pathways are simultaneous activated under cholestasis background. It is hoped that the RNA-sequencing results and bioinformation analysis in the present study could contribute some indications for description of this pathological process.

There are some limitation to the present study; first, as in any statistical analysis, a reliable result depends on large-scale samples. The sample size in the present study was relatively small, due to the rare incidence of this progressive and severe neonatal fibro-obstructive cholangiopathy. Second, two age-unmatched patients with choledochal cyst under normal liver function test was as control instead of normal liver tissues due to ethical issues. It is hoped that further studies can be performed to validate the findings of the present study by enrolling more clinical samples and then the possible mechanisms can be clarified more accurately. Third, experiments on these candidate hub genes and pathways of the potential relation pair and network crosstalking to elucidate the molecular mechanism of BA are required.

Acknowledgements

Not applicable.

Funding

The present study was supported by the National Natural Science Foundation of China under (grant no. 81770512), Science, Technology and Innovation Commission of Shenzhen Municipality under (grant no. JCYJ20210324134202007) and Sanming Project of Medicine in Shenzhen under Grant (grant no. SZSM201812055).

Availability of data and materials

The data generated and analyzed in the present study may be found in the Sequence Read Archive (SRA) under accession number (SUB7923751) at the following URL: https://www.ncbi.nlm.nih.gov/sra/PRJNA701623 and the GSE46960 dataset obtained from GEO at https://www.ncbi.nlm.nih.gov/geo/query/acc.cgi?acc=GSE46960. Other data used and/or analyzed during the current study are available from the corresponding author on reasonable request.

Authors' contributions

YY and BW confirm the authenticity of all the raw data. TL and BW conceived and designed the present study. YY collected liver tissues and clinical data. YY and WeiW performed the experiments. WenW and WeiW analyzed the data. YY and WenW interpreted the data. WenW and WeiW drafted the manuscript. WenW and TL prepared Fig. 1-7 and Tables II and III. YY and WeiW prepared Table I. YY, TL and BW reviewed and revised the manuscript. All authors read and approved the final manuscript.

Ethics approval and consent to participate

The study was approved by Ethics Committee on Human Research of the Faculty of the Shenzhen Children's Hospital (approval no. 202106602). All tissue samples were collected with written informed consent from all participants or parents/guardians in the case of children under 18 and was conducted based on the principles expressed in the 1975 Declaration of Helsinki.

Patient consent for publication

Not applicable.

Competing interests

The authors declare that they have no competing interests.

References

1. Hartley JL, Davenport M and Kelly DA: Biliary atresia. Lancet 374: 1704-1713, 2009.
2. Shen WJ, Chen G, Wang M and Zheng S: Liver fibrosis in biliary atresia. World J Pediatr 15: 117-123, 2019.
3. Haafiz AB: Liver fibrosis in biliary atresia. Expert Rev Gastroenterol Hepatol 4: 335-343, 2010.
4. Pereira TN, Lewindon PJ, Greer RM, Hoskins AC, Williamson RM, Shepherd RW and Ramm GA: Transcriptional basis for hepatic fibrosis in cystic fibrosis-associated liver disease. J Pediatr Gastroenterol Nutr 54: 328-335, 2012.
5. Xiao J, Xia SY, Xia Y, Xia Q and Wang XR: Transcriptome profiling of biliary atresia from new born infants by deep sequencing. Mol Biol Rep 41: 8063-8069, 2014.
6. Dong R, Yang Y, Shen Z, Zheng C, Jin Z, Huang Y, Zhang Z, Zheng S and Chen G: Forkhead box A3 attenuated the progression of fibrosis in a rat model of biliary atresia. Cell Death Dis 8: e2719, 2017.
7. Liu C, Chiu JH, Chin T, Wang LS, Li AF, Chow KC and Wei C: Expression of fas ligand on bile ductule epithelium in biliary atresia-a poor prognostic factor. J Pediatr Surg 35: 1591-1596, 2000.
8. Ramachandran P, Balamurali D, Peter JJ, Kumar MM, Safwan M, Vij M, Rela M and Mahalingam S: RNA-seq reveals outcome-specific gene expression of MMP7 and PCK1 in biliary atresia. Mol Biol Rep 46: 5123-5130, 2019.
9. Gilmore TD: The Rel/NF-kappaB signal transduction pathway: Introduction. Oncogene 18: 6842-6844, 1999.
10. Wang C, Ma C, Gong L, Guo Y, Fu K, Zhang Y, Zhou H and Li Y: Macrophage polarization and its role in liver disease. Front Immunol 12: 803037, 2021.
11. Yoo W, Lee J, Noh KH, Lee S, Jung D, Kabir MH, Park D, Lee C, Kwon KS, Kim JS and Kim S: Progranulin attenuates liver fibrosis by downregulating the inflammatory response. Cell Death Dis 10: 758, 2019.

12. Chen L, Goryachev A, Sun J, Kim P, Zhang H, Phillips MJ, Macgregor P, Lebel S, Edwards AM, Cao Q and Furuya KN: Altered expression of genes involved in hepatic morphogenesis and fibrogenesis are identified by cDNA microarray analysis in biliary atresia. Hepatology 38: 567-576, 2003.
13. Luo Z, Shivakumar P, Mourya R, Gutta S and Bezerra JA: Gene expression signatures associated with survival times of pediatric patients with biliary atresia identify potential therapeutic agents. Gastroenterology 157: 1138-1152.e14, 2019.
14. Zhu J, Fu H, Wu Y and Zheng X: Function of lncRNAs and approaches to lncRNA-protein interactions. Sci China Life Sci 56: 876-885, 2013.
15. Peng H, Wan LY, Liang JJ, Zhang YQ, Ai WB and Wu JF: The roles of lncRNA in hepatic fibrosis. Cell Biosci 8: 63, 2018.
16. Dong BS, Shi MJ, Su SB and Zhang H: Insight into long noncoding competing endogenous RNA networks in hepatic fibrosis: The potential implications for mechanism and therapy. Gene 687: 255-260, 2019.
17. Xiao Y, Liu R, Li X, Gurley EC, Hylemon PB, Lu Y, Zhou H and Cai W: Long noncoding RNA H19 contributes to cholangiocyte proliferation and cholestatic liver fibrosis in biliary atresia. Hepatology 70: 1658-1673, 2019.
18. Nuerzhati Y, Dong R, Song Z and Zheng S: Role of the long non-coding RNA-Annexin A2 pseudogene 3/Annexin A2 signaling pathway in biliary atresia-associated hepatic injury. Int J Mol Med 43: 739-748, 2019.
19. Ye Y, Wu W, Zheng J, Zhang L and Wang B: Role of long non-coding RNA-adducin 3 antisense RNA1 in liver fibrosis of biliary atresia. Bioengineered 13: 6222-6230, 2022.
20. Jiang H, Wu F, Jiang N, Gao J and Zhang J: Reconstruction and analysis of competitive endogenous RNA network reveals regulatory role of long non-coding RNAs in hepatic fibrosis. Mol Med Rep 20: 4091-4100, 2019.
21. Chen W, Chen X, Wang Y, Liu T, Liang Y, Xiao Y and Chen L: Construction and analysis of lncRNA-mediated ceRNA network in cervical squamous cell carcinoma by weighted gene Co-Expression Network Analysis. Med Sci Monit 25: 2609-2622, 2019.
22. Song J, Ye A, Jiang E, Yin X, Chen Z, Bai G, Zhou Y and Liu J: Reconstruction and analysis of the aberrant lncRNA-miRNA-mRNA network based on competitive endogenous RNA in CESC. J Cell Biochem 119: 6665-6673, 2018.
23. Kilgore A and Mack CL: Update on investigations pertaining to the pathogenesis of biliary atresia. Pediatr Surg Int 33: 1233-1241, 2017.
24. Filmus J and Capurro M: Glypican-3: A marker and a therapeutic target in hepatocellular carcinoma. FEBS J 280: 2471-2476, 2013.
25. Song HH, Shi W, Xiang YY and Filmus J: The loss of glypican-3 induces alterations in Wnt signaling. J Biol Chem 280: 2116-2125, 2005.
26. Bhave VS, Mars W, Donthamsetty S, Zhang X, Tan L, Luo J, Bowen WC and Michalopoulos GK: Regulation of liver growth by glypican 3, CD81, hedgehog, and Hhex. Am J Pathol 183: 153-159, 2013.
27. Midorikawa Y, Ishikawa S, Iwanari H, Imamura T, Sakamoto H, Miyazono K, Kodama T, Makuuchi M and Aburatani H: Glypican-3, overexpressed in hepatocellular carcinoma, modulates FGF2 and BMP-7 signaling. Int J Cancer 103: 455-465, 2003.
28. Decaens T, Godard C, de Reyniès A, Rickman DS, Tronche F, Couty JP, Perret C and Colnot S: Stabilization of beta-catenin affects mouse embryonic liver growth and hepatoblast fate. Hepatology 47: 247-258, 2008.
29. Sirisomboonlarp K, Udomsinprasert W, McConachie E, Woraruthai T, Poovorawan Y and Honsawek S: Increased serum glypican-3 is associated with liver stiffness and hepatic dysfunction in children with biliary atresia. Clin Exp Hepatol 5: 48-54, 2019.
30. Galle PR, Foerster F, Kudo M, Chan SL, Llovet JM, Qin S, Schelman WR, Chintharlapalli S, Abada PB, Sherman M and Zhu AX: Biology and significance of alpha-fetoprotein in hepatocellular carcinoma. Liver Int 39: 2214-2229, 2019.
31. Schneider DT, Calaminus G and Göbel U: Diagnostic value of alpha 1-fetoprotein and beta-human chorionic gonadotropin in infancy and childhood. Pediatr Hematol Oncol 18: 11-26, 2001.
32. Amir AZ, Sharma A, Cutz E, Avitzur Y, Shaikh F, Kamath BM, Ling SC, Ghanekar A and Ng VL: Hepatoblastoma in explanted livers of patients with biliary atresia. J Pediatr Gastroenterol Nutr 63: 188-194, 2016.
33. Yoon HJ, Jeon TY, Yoo SY, Kim JH, Eo H, Lee SK and Kim JS: Hepatic tumours in children with biliary atresia: Single-centre experience in 13 cases and review of the literature. Clin Radiol 69: e113-e119, 2014.
34. Balistreri WF: Neonatal cholestasis. J Pediatr 106: 171-184, 1985.
35. Shteyer E, Lalazar G, Hemed N, Pappo O, Granot E, Yerushalmi B and Gross E: Continuous 13C-methacetin breath test differentiates biliary atresia from other causes of neonatal cholestasis. J Pediatr Gastroenterol Nutr 56: 60-65, 2013.
36. Ilan Y: Review article: The assessment of liver function using breath tests. Aliment Pharmacol Ther 26: 1293-1302, 2007.
37. Braden B, Faust D, Sarrazin U, Zeuzem S, Dietrich CF, Caspary WF and Sarrazin C: 13C-methacetin breath test as liver function test in patients with chronic hepatitis C virus infection. Aliment Pharmacol Ther 21: 179-185, 2005.
38. Nakai K, Tanaka H, Hanada K, Ogata H, Suzuki F, Kumada H, Miyajima A, Ishida S, Sunouchi M, Habano W, *et al*: Decreased expression of cytochromes P450 1A2, 2E1, and 3A4 and drug transporters Na+-taurocholate-cotransporting polypeptide, organic cation transporter 1, and organic anion-transporting peptide-C correlates with the progression of liver fibrosis in chronic hepatitis C patients. Drug Metab Dispos 36: 1786-1793, 2008.
39. Zhu Q, Huang C, Meng X and Li J: CYP1A2 contributes to alcohol-induced abnormal lipid metabolism through the PTEN/AKT/SREBP-1c pathway. Biochem Biophys Res Commun 513: 509-514, 2019.
40. Crawford JH, Yang S, Zhou M, Simms HH and Wang P: Down-regulation of hepatic CYP1A2 plays an important role in inflammatory responses in sepsis. Crit Care Med 32: 502-508, 2004.
41. Makhmudi A, Supanji R, Putra BP and Gunadi: The effect of APTR, Fn14 and CD133 expressions on liver fibrosis in biliary atresia patients. Pediatr Surg Int 36: 75-79, 2020.
42. Yu F, Lu Z, Cai J, Huang K, Chen B, Li G, Dong P and Zheng J: MALAT1 functions as a competing endogenous RNA to mediate Rac1 expression by sequestering miR-101b in liver fibrosis. Cell Cycle 14: 3885-3896, 2015.
43. Makhmudi A, Kalim AS and Gunadi: microRNA-21 expressions impact on liver fibrosis in biliary atresia patients. BMC Res Notes 12: 189, 2019.
44. Zheng L, Lv Z, Gong Z, Sheng Q, Gao Z, Zhang Y, Yu S, Zhou J, Xi Z and Wang X: Fn14 hepatic progenitor cells are associated with liver fibrosis in biliary atresia. Pediatr Surg Int 33: 593-599, 2017.
45. Chu X, Jin Q, Chen H, Wood GC, Petrick A, Strodel W, Gabrielsen J, Benotti P, Mirshahi T, Carey DJ, *et al*: CCL20 is up-regulated in non-alcoholic fatty liver disease fibrosis and is produced by hepatic stellate cells in response to fatty acid loading. J Transl Med 16: 108, 2018.
46. Zou X, Ramachandran P, Kendall TJ, Pellicoro A, Dora E, Aucott RL, Manwani K, Man TY, Chapman KE, Henderson NC, *et al*: 11Beta-hydroxysteroid dehydrogenase-1 deficiency or inhibition enhances hepatic myofibroblast activation in murine liver fibrosis. Hepatology 67: 2167-2181, 2018.
47. Nikolaou N, Gathercole LL, Marchand L, Althari S, Dempster NJ, Green CJ, van de Bunt M, McNeil C, Arvaniti A, Hughes BA, *et al*: AKR1D1 is a novel regulator of metabolic phenotype in human hepatocytes and is dysregulated in non-alcoholic fatty liver disease. Metabolism 99: 67-80, 2019.
48. Fernández-Álvarez S, Gutiérrez-de Juan V, Zubiete-Franco I, Barbier-Torres L, Lahoz A, Parés A, Luka Z, Wagner C, Lu SC, Mato JM, *et al*: TRAIL-producing NK cells contribute to liver injury and related fibrogenesis in the context of GNMT deficiency. Lab Invest 95: 223-236, 2015.
49. Xie ZY, Wang FF, Xiao ZH, Liu SF, Lai YL and Tang SL: Long noncoding RNA XIST enhances ethanol-induced hepatic stellate cells autophagy and activation via miR-29b/HMGB1 axis. IUBMB Life 71: 1962-1972, 2019.
50. Yan F, Wang X and Zeng Y: 3D genomic regulation of lncRNA and Xist in X chromosome. Semin Cell Dev Biol 90: 174-180, 2019.
51. Kerola A, Lohi J, Heikkilä P, Mutanen A, Jalanko H and Pakarinen MP: Divergent expression of liver transforming growth factor superfamily cytokines after successful portoenterostomy in biliary atresia. Surgery 165: 905-911, 2019.
52. Zhang H, Meng H, Huang X, Tong W, Liang X, Li J, Zhang C and Chen M: lncRNA MIR4435-2HG promotes cancer cell migration and invasion in prostate carcinoma by upregulating TGF-β1. Oncol Lett 18: 4016-4021, 2019.

53. Yang M, He X, Huang X, Wang J, He Y and Wei L: LncRNA MIR4435-2HG-mediated upregulation of TGF-β1 promotes migration and proliferation of nonsmall cell lung cancer cells. Environ Toxicol 35: 582-590, 2020.
54. Gong J, Xu X, Zhang X and Zhou Y: LncRNA MIR4435-2HG is a potential early diagnostic marker for ovarian carcinoma. Acta Biochim Biophys Sin (Shanghai) 51: 953-959, 2019.
55. Overbeek SA, Braber S, Koelink PJ, Henricks PAJ, Mortaz E, Loi ATL, Jackson PL, Garssen J, Wagenaar GTM, Timens W, *et al*: Cigarette smoke-induced collagen destruction; key to chronic neutrophilic airway inflammation? PLoS One 8: e55612, 2013.
56. Dong R and Zheng S: Interleukin-8: A critical chemokine in biliary atresia. J Gastroenterol Hepatol 30: 970-976, 2015.
57. Arafa RS, Haie OMA, El-Azab DS, Abdel-Rahman AM and Sira MM: Significant hepatic expression of IL-2 and IL-8 in biliary atresia compared with other neonatal cholestatic disorders. Cytokine 79: 59-65, 2016.
58. Saito T, Hishiki T, Terui K, Mitsunaga T, Terui E, Nakata M and Yoshida H: Toll-like receptor mRNA expression in liver tissue from patients with biliary atresia. J Pediatr Gastroenterol Nutr 53: 620-626, 2011.
59. Wu Y, Liu T, Yuan Y and Zhang Z: Gene expression profile of TLR7 signaling pathway in the liver of rhesus rotavirus-induced murine biliary atresia. Biochem Biophys Res Commun 503: 291-296, 2018.
60. Huang YH, Chou MH, Du YY, Huang CC, Wu CL, Chen CL and Chuang JH: Expression of toll-like receptors and type 1 interferon specific protein MxA in biliary atresia. Lab Invest 87: 66-74, 2007.
61. Baba H, Ohtsuka Y, Fujii T, Haruna H, Nagata S, Kobayashi H, Yamataka A, Shimizu T, Miyano T and Yamashiro Y: Immunological investigation of the hepatic tissue from infants with biliary atresia. Pediatr Surg Int 25: 157-162, 2009.
62. Leonhardt J, Stanulla M, von Wasielewski R, Skokowa J, Kübler J, Ure BM and Petersen C: Gene expression profile of the infective murine model for biliary atresia. Pediatr Surg Int 22: 84-89, 2006.
63. De Bock L, Boussery K, Van Winckel M, Paepe PD, Rogiers X, Stephenne X, Sokal E and Bocxlaer JV: In vitro cytochrome p450 activity decreases in children with high pediatric end-stage liver disease scores. Drug Metab Dispos 41: 390-397, 2013.